EGF- or PDGF-triggered activation of Ras. This is reminiscent of mice deficient in the Eps8 activator component of the Rac-GEF complex Eps8/E3b1/Sos-1 (ref. 25). PI(3)K- and Ras-dependent ruffling is impaired in the mutant, yet the mice are phenotypically healthy. Thus, indications exist *in vivo* for redundancies in Rac-dependent signalling of cytoskeletal rearrangements. □

Methods

Plasmids

KIAA0640 complementary DNA was provided by T. Nagase (Kazusa DNA Research Institute). For GFP–SWAP-70 expression in mammalian cells, cDNA of SWAP-70 was subcloned into pEGFP C1 (Clontech). Point mutations were induced by the QuickChange site-directed mutagenesis method (Stratagene). For the SWAP-70 (R230C and K291A) mutants, 5′-AAAACTGGACTGAATGTTGGTTTGTTTTAAAACCCAA-3′ and 5′-GATAAGACTTTTGAAATCAGTGCTAGCGATGCGAAGAAGAAACAGGAGTGGATT CAA-3′ were used as sense primers, respectively. For deletion mutants, cDNAs coding for different segments were inserted into pEGFP C1. pEFBOS HA–RasN17, pEFBOS HA–RasV12 and pEFBOS HA–Rac were gifts from K. Kaibuchi. pCMV HA–MAPK was provided by Y. Gotoh. cDNA of the GEF domain of human Sos1 was cloned by reverse-transcriptase-mediated polymerase chain reaction.

Protein purification and peptide sequence analysis

SWAP-70 purification from bovine brain with the use of PtdIns(3,4,5)P_3-APB beads and amino-acid sequencing were done as described[12,26].

Transfection

Transfection of COS7 cells was performed by electroporation. Cells were suspended in 500 μl of K-PBS (30.8 mM NaCl, 120.7 mM KCl, 8.1 mM Na_2HPO_4, 1.46 mM KCl, 5 mM $MgCl_2$) containing 20 μg DNA and were pulsed with a Cell-porator (Gibco BRL) at 800 μF capacitance and 240 V. Transfection of NIH 3T3 cells was done by electroporation as described above or by lipofection with LipofectAMINE (Gibco-BRL). Transfection of 293T cells was done as described previously[27]. Introduction of the DNA to cultivated kidney cells was done by microinjection as described previously[28] or by lipofection.

Fluorescence microscopy

Cells were stained for F-actin with tetramethylrhodamine-isothiocyanate-conjugated phalloidin as described previously[28]. Cells were examined by confocal fluorescence microscopy (Olympus IX-70).

GDP release assay for Rac, binding of SWAP-70 to Rac, and Rac activation assay

The GDP release assay was performed as described[29]. Binding of SWAP-70 to Rho GTPases was performed as described previously[30]. For the Rac1 (or Cdc42) activation assay, Rac1 (or Cdc42) was expressed in NIH 3T3, COS7 or primary kidney cells together with wild-type or mutant SWAP-70. Cells were treated for 5 min with or without PDGF or EGF, washed with ice-cold PBS containing 5 mM $MgCl_2$, lysed in lysis buffer (50 mM Tris-HCl pH 7.5, 1% (v/v) Triton X-100, 150 mM NaCl, 10% (v/v) glycerol, 2 mM dithiothreitol, 10 mM $MgCl_2$) and centrifuged for 10 min at 15,000*g* at 4 °C. Supernatants were incubated for 30 min at 4 °C with GST–Cdc4^2/Rac interactive binding (CRIB) (from PAK1), prebound to glutathione–Sepharose beads. Beads were washed, and bound material was analysed by SDS–polyacrylamide gel electrophoresis and immunoblotting.

Received 9 October 2001; accepted 11 February 2002.

1. Toker, A. & Cantley, L. C. Signalling through the lipid products of phosphoinositide-3-OH kinase. *Nature* **387,** 673–676 (1997).
2. Downward, J. Role of phosphoinositide-3-OH kinase in Ras signaling. *Adv. Second Mess. Phosphoprot. Res.* **31,** 1–10 (1997).
3. Martin, T. F. Phosphoinositide lipids as signaling molecules: Common themes for signal transduction, cytoskeletal regulation, and membrane trafficking. *Annu. Rev. Cell. Dev. Biol.* **14,** 231–264 (1998).
4. Rameh, L. E. & Cantley, L. C. The role of phosphoinositide 3-kinase lipid products in cell function. *J. Biol. Chem.* **274,** 8347–8350 (1999).
5. Fruman, D. A., Meyers, R. E. & Cantley, L. C. Phosphoinositide kinases. *Annu. Rev. Biochem.* **67,** 481–507 (1998).
6. Fukui, Y., Ihara, S. & Nagata, S. Downstream of phosphatidylinositol-3 kinase, a multifunctional signaling molecule, and its regulation in cell responses. *J. Biochem. (Tokyo)* **124,** 1–7 (1998).
7. Vanhaesebroeck, B. *et al.* Synthesis and function of 3-phosphorylated inositol lipids. *Annu. Rev. Biochem.* **70,** 535–602 (2001).
8. Borggrefe, T., Wabl, M., Akhmedov, A. T. & Jessberger, R. A B-cell-specific DNA recombination complex. *J. Biol. Chem.* **273,** 17025–17035 (1998).
9. Borggrefe, T. *et al.* Cellular, intracellular, and developmental expression patterns of murine SWAP-70. *Eur. J. Immunol.* **29,** 1812–1822 (1999).
10. Masat, L. *et al.* Association of SWAP-70 with the B cell antigen receptor complex. *Proc. Natl Acad. Sci. USA* **97,** 2180–2184 (2000).
11. Borggrefe, T., Keshavarzi, S., Gross, B., Wabl, M. & Jessberger, R. Impaired IgE response in SWAP-70-deficient mice. *Eur. J. Immunol.* **8,** 2467–2475 (2001).
12. Shirai, R. *et al.* Synthesis of diacylglycerol analogs of phosphatidylinositol 3,4,5-trisphosphate. *Tetrahedron Lett.* **39,** 9485–9488 (1998).
13. Staal, S. Molecular cloning of the *akt* oncogene and its human homologues AKT1 and AKT2: amplification of AKT1 in a primary human gastric adenocarcinoma. *Proc. Natl Acad. Sci. USA* **84,** 5034–5037 (1987).
14. Tanaka, K. *et al.* A target of phosphatidylinositol 3,4,5-trisphosphate with a zinc finger motif similar to that of the ADP-ribosylation-factor GTPase-activating protein and two pleckstrin homology domains. *Eur. J. Biochem.* **245,** 512–519 (1997).
15. Maekawa, M. *et al.* A novel mammalian Ras GTPase-activating protein which has phospholipid-binding and Btk homology regions. *Mol. Cell. Biol.* **14,** 6879–6885 (1994).
16. Campbell, D. & Kernan, J. Mast cells in the central nervous system. *Nature* **210,** 756–757 (1966).
17. Thomas, J. *et al.* Colocalization of X-linked agammaglobulinemia and X-linked immunodeficiency genes. *Science* **261,** 355–358 (1993).
18. Han, J. *et al.* Role of substrates and products of PI 3-kinase in regulating activation of Rac-related guanosine triphosphatases by Vav. *Science* **279,** 558–560 (1998).
19. Fleming, I. N., Gray, A. & Downes, C. P. Regulation of the Rac1-specific exchange factor Tiam1 involves both phosphoinositide 3-kinase-dependent and -independent components. *Biochem. J.* **351,** 173–182 (2000).
20. Das, B. *et al.* Control of intramolecular interactions between the pleckstrin homology and Dbl homology domains of Vav and Sos1 regulates Rac binding. *J. Biol. Chem.* **275,** 15074–15081 (2000).
21. Joly, M., Kazlauskas, A., Fay, F. S. & Corvera, S. Disruption of PDGF receptor trafficking by mutation of its PI-3 kinase binding sites. *Science* **263,** 684–687 (1994).
22. Martin, S. S. *et al.* Phosphatidylinositol 3-kinase is necessary and sufficient for insulin-stimulated stress fiber breakdown. *Endocrinology* **137,** 5045–5054 (1996).
23. Wennstrom, S. & Downward, J. Role of phosphoinositide 3-kinase in activation of ras and mitogen-activated protein kinase by epidermal growth factor. *Mol. Cell. Biol.* **19,** 4279–4288 (1999).
24. Missy, K. *et al.* Lipid products of phosphoinositide 3-kinase interact with Rac1 GTPase and stimulate GDP dissociation. *J. Biol. Chem.* **273,** 30279–30286 (1998).
25. Scita, G. *et al.* EPS8 and E3B1 transduce signals from Ras to Rac. *Nature* **401,** 290–293 (1999).
26. Iwamatsu, A. S-carboxymethylation of proteins transferred onto polyvinylidene difluoride membranes followed by *in situ* protease digestion and amino acid microsequencing. *Electrophoresis* **13,** 142–147 (1992).
27. Tanaka, K. *et al.* Evidence that a phosphatidylinositol 3,4,5-trisphosphate-binding protein can function in nucleus. *J. Biol. Chem.* **274,** 3919–3922 (1999).
28. Kita, Y. *et al.* Microinjection of activated phosphatidylinositol-3 kinase induces process outgrowth in rat PC12 cells through the Rac-JNK signal transduction pathway. *J. Cell Sci.* **111,** 907–915 (1998).
29. Lenzen, C., Cool, R. & Wittinghofer, A. Analysis of intrinsic and CDC25-stimulated guanine nucleotide exchange of p21ras-nucleotide complexes by fluorescence measurements. *Methods Enzymol.* **255,** 95–109 (1995).
30. Zheng, Y., Bagrodia, S. & Cerione, R. Activation of phosphoinositide 3-kinase activity by Cdc42Hs binding to p85. *J. Biol. Chem.* **269,** 18727–18730 (1994).
31. Gross, B. *et al.* SWAP-70 deficient mast cells are impaired in development and IgE-mediated degranulation. *Eur. J. Immunol.* (in the press).

Supplementary Information accompanies the paper on *Nature's* website (http://www.nature.com).

Acknowledgements

We thank B. Mayer and M. Matsuda for useful suggestions and critical reading of the manuscript, and T. Nagase (Kazusa DNA Research Institute) for supplying the KIAA0640 clone. This work was supported by grants-in-aid for scientific research to Y.F. from the Ministry of Education, Science, Sports, and Culture of Japan, and by an NIH grant to R.J.

Competing interests statement

The authors declare that they have no competing financial interests.

Correspondence and requests for materials should be addressed to Y.F. (e-mail: ayfukui@mail.ecc.u-tokyo.ac.jp).

A proteasomal ATPase subunit recognizes the polyubiquitin degradation signal

Y. Amy Lam*, T. Glen Lawson†, Murugesan Velayutham‡, Jay L. Zweier‡ & Cecile M. Pickart*

** Department of Biochemistry and Molecular Biology, School of Public Health; and ‡ Department of Medicine and EPR Center, School of Medicine, Johns Hopkins University, Baltimore, Maryland, USA*
† Department of Chemistry, Bates College, Lewiston, Maine 04240, USA

The 26S proteasome is the chief site of regulatory protein turnover in eukaryotic cells[1]. It comprises one 20S catalytic complex (composed of four stacked rings of seven members) and two axially positioned 19S regulatory complexes (each containing about 18 subunits) that control substrate access to the catalytic

chamber[2]. In most cases, targeting to the 26S proteasome depends on tagging of the substrate with a specific type of polyubiquitin chain[3–6]. Recognition of this signal is followed by substrate unfolding and translocation, which are presumably catalysed by one or more of six distinct AAA ATPases located in the base—a ring-like 19S subdomain that abuts the axial pore of the 20S complex and exhibits chaperone activity *in vitro*[7–9]. Despite the importance of polyubiquitin chain recognition in proteasome function, the site of this signal's interaction with the 19S complex has not been identified previously. Here we use crosslinking to a reactive polyubiquitin chain to show that a specific ATPase subunit, S6′ (also known as Rpt5), contacts the bound chain. The interaction of this signal with 26S proteasomes is modulated by ATP hydrolysis. Our results suggest that productive recognition of the proteolytic signal, as well as proteasome assembly and substrate unfolding, are ATP-dependent events.

We used intact 26S proteasomes—proteases with a relative molecular mass of 2,100,000 (M_r 2,100K)—as the starting point to identify, by means of crosslinking, the subunit(s) of the 19S complex that contacts the bound polyubiquitin chain. To construct a reactive version of tetra-ubiquitin (Ub_4), which is the minimal signal for efficient targeting to proteasomes[6], we took advantage of the absence of endogenous cysteines in ubiquitin and our previous finding that a P37C mutation is permissive for chain recognition[10]. We placed the ubiquitin P37C mutant at the proximal position in Ub_4, and then introduced a radio-iodinated photoreactive crosslinker (APDP) at Cys 37 via disulphide exchange (Fig. 1). The reactive group was thus positioned near the proximal Leu 8 (refs 11, 12), whose side chain is necessary for optimal recognition of Ub_4 by 26S proteasomes[6,13].

Purified bovine 26S proteasomes were pre-incubated with a stoichiometric concentration (relative to the 19S complex) of the reactive chain, irradiated with ultraviolet radiation, and resolved by SDS–polyacrylamide gel electrophoresis (PAGE) under reducing conditions to visualize crosslinked partner(s) at their normal molecular masses (Fig. 1). Despite the presence of approximately 18 distinct polypeptides in the 19S complex, there were only three significant crosslinked products, indicating substantial specificity of interaction (Fig. 2a, lane 6). The most abundant product was derived from intramolecular crosslinking, as it co-migrated with Ub_4 and was seen in the absence of proteasomes (Fig. 2a; $*Ub_4$, lane 3 and 6). Reactions containing proteasomes and reactive Ub_4 uniquely yielded radiolabelled bands with molecular masses of roughly 48K and 50K (lane 6). The masses of these two proteins are consistent with identification as subunits of the 19S complex[2]. Crosslinking of both proteins depended strictly on ultraviolet irradiation (not shown), and neither protein crosslinked to Ub_1 (lane 5), which does not bind detectably to proteasomes[6]. Reaction of the 50K protein, but not the smaller protein, was competed efficiently by unlabelled wild-type Ub_4 (Fig. 2a, compare lanes 8 and 6, and b), but not by a mutant Ub_4 that does not bind to proteasomes[10] (Fig. 2a, compare lanes 9 and 6). Only the 50K

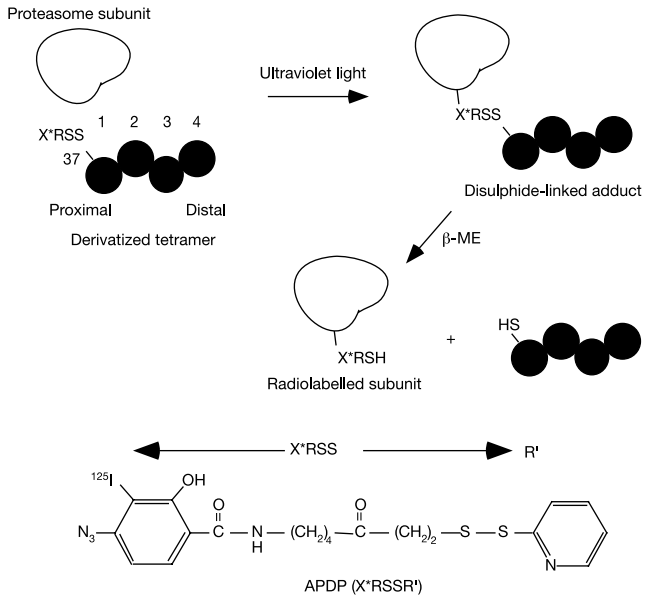

Figure 1 Crosslinking strategy. ^{125}I-labelled APDP was linked to Cys 37 in the proximal ubiquitin of Ub_4 by means of disulphide exchange (1 and 4 denote proximal and distal ubiquitins, respectively). As in the natural chain signal[3,4], the ubiquitins are linked by Lys 48–Gly 76 isopeptide bonds[27]. After ultraviolet activation in the presence of proteasomes, the nitrene group of APDP crosslinks to a 19S subunit that is in close spatial proximity. Treatment of this initial crosslinked product with β-mercaptoethanol (β-ME) releases the (unlabelled) chain.

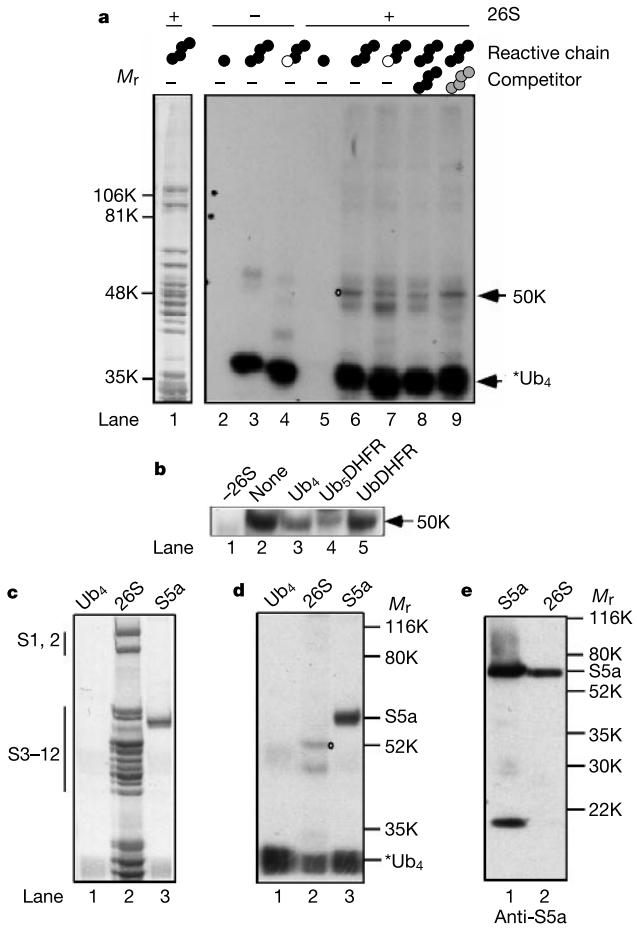

Figure 2 Specific crosslinking of Ub_4 to proteasomes. **a**, The 50K proteasome subunit crosslinks to Ub_4. Crosslinking reactions (0.5 mM Mg-ATP) contained the indicated reactive species (Ub_1, wild-type Ub_4, or Ub_4 with proximal ubiquitin L8A (white circles)). Black circles, wild-type ubiquitin; grey circles, L8A,I44A-ubiquitin. Lane 1, Coomassie stain of lane 6; lanes 2–9, autoradiograph. Lane 8 shows competition by unlabelled wild-type Ub_4; lane 9 shows competition by L8A, I44A Ub_4 (5 μM each). The 50K band is indicated by a dot in the autoradiograph. $*Ub_4$, product of intramolecular crosslinking (identical migration of this band on a non-reducing gel excluded its origin in an intermolecular reaction). **b**, The indicated competitors were added at 10 μM each. **c**, Coomassie stain of Ub_4 crosslinking reactions with 1 μM proteasomes or S5a (ref. 13) (2 mM Mg-ATP). Ub_4 denotes reaction with chain alone; S1, 2 and S3–12 denote subunits of the 19S complex. **d**, Autoradiograph of **c**. **e**, Anti-S5a western blot.

band showed diminished reaction when the L8A mutation was introduced into the proximal ubiquitin of the reactive chain (Fig. 2a, compare lanes 6 and 7)—an alteration that diminishes by several-fold the affinity of Ub_4 for proteasomes[6]. Of note, crosslinking by wild-type Ub_4 was competed efficiently by Ub_5-dihydrofolate reductase (DHFR), a polyubiquitinated substrate with high affinity for proteasomes[6], but not by UbDHFR, which does not bind detectably[6] (Fig. 2b). Thus, only the 50K protein behaved as expected for an authentic polyubiquitin recognition factor, whose crosslinking should be sensitive to chain length, competed by an authentic substrate, and dependent on a hydrophobic contact with ubiquitin Leu 8 (ref. 6). To exclude the possibility that the 50K subunit was adjacent to a primary binding protein and reacted only owing to the long linker arm of APDP, we showed that the 50K subunit still crosslinked when we moved APDP to the distal ubiquitin in the chain (not shown).

Purified S5a (also known as Rpn10), an approximately 50K subunit of the 19S complex, avidly binds polyubiquitin chains[13,14]. Not surprisingly, purified recombinant S5a (Fig. 2c, lane 3) also crosslinked strongly to the reactive chain (Fig. 2d). However, although S5a was present in the proteasome preparation (Fig. 2e), the crosslinked 50K protein in the 19S complex was not S5a, as shown by distinct mobilities of the respective crosslinked products (Fig. 2d, compare lanes 2 and 3). These results suggest that interactions between neighbours within the 19S complex occlude the polyubiquitin-binding site of S5a, and indicate that isolated S5a exhibits properties that are not manifested when this subunit is part of the 19S complex. The current results may explain the dispensability of the polyubiquitin-binding site of S5a subunits for the degradation of most polyubiquitinated substrates in yeast cells[15,16].

The 50K polyubiquitin-interacting protein in the 19S complex displayed an isoelectric point (pI) of roughly 5 on a two-dimensional IEF/SDS–PAGE gel (not shown). The only known 19S subunits with these physical properties are the ATPases S6′ (also known as Rpt5 and TBP1) and S6 (also known as Rpt3 and TBP7)[2], which are thought to be located at adjacent positions in the presumptive ATPase ring[17,18]. Peptide sequencing revealed that both S6 and S6′ co-migrated with the labelled band (not shown). To determine which ATPase(s) was targeted by the reactive chain, we took advantage of the fact that the chain and its interaction partner are initially linked by a disulphide bond (Fig. 1). Thus, a fraction of the relevant ATPase(s) should migrate with an apparent mass of about 80K in non-reducing SDS–PAGE, and this form should be immunochemically detectable using antibodies that distinguish the two ATPases (Fig. 3a, modulator complex lacks S6 (ref. 19). As shown in Fig. 3b, only the S6′ antibody detected an 80K band in non-reducing SDS–PAGE of crosslinked proteasomes. Consistent with the identification of this band as a disulphide-linked adduct of S6′ and Ub_4, it reacted with ubiquitin antibodies (Fig. 3c) and the principal fraction of the S6′/ubiquitin immunoreactivity disappeared after reduction (Fig. 3b, c, compare lanes 6 and 4). Therefore S6′ ATPase within the 26S proteasome contacts

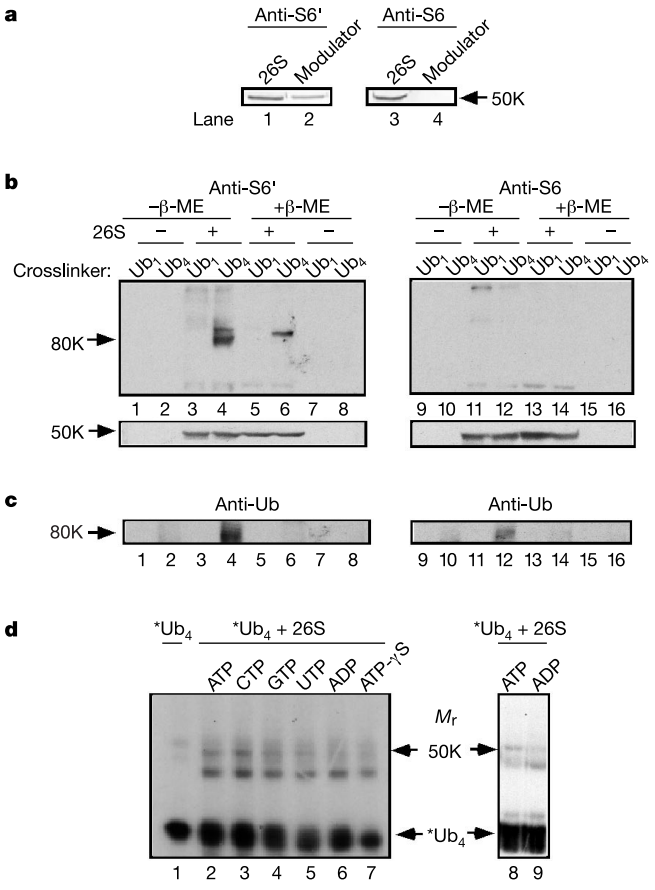

Figure 3 The 50K crosslinked protein is S6′. **a**, S6 and S6′ antibodies do not crossreact. A western analysis of 26S proteasomes (lanes 1, 3) or equimolar modulator, a small complex that lacks S6 (ref. 19; lanes 2, 4), is shown. **b**, S6′, but not S6, is initially linked to reactive Ub_4 by a disulphide bond (western blots). Crosslinking reactions with reactive Ub_1 or Ub_4 (2 mM Mg-ATP) were quenched in SDS with or without β-mercaptoethanol (β-ME). Sections of the blot corresponding to greater than 60K (top panel) and about 50K (bottom panel) were analysed separately. **c**, The 80K complex contains ubiquitin (anti-ubiquitin western blots; the top panels from **b** were stripped and re-probed). **d**, Efficient crosslinking requires ATP hydrolysis (autoradiograph). 26S proteasomes were depleted of ATP before crosslinking with reactive Ub_4 plus the indicated nucleotide (2 mM, with 10 mM $MgCl_2$). Lanes 8 and 9 show an independent experiment. *Ub_4, product of intramolecular crosslinking.

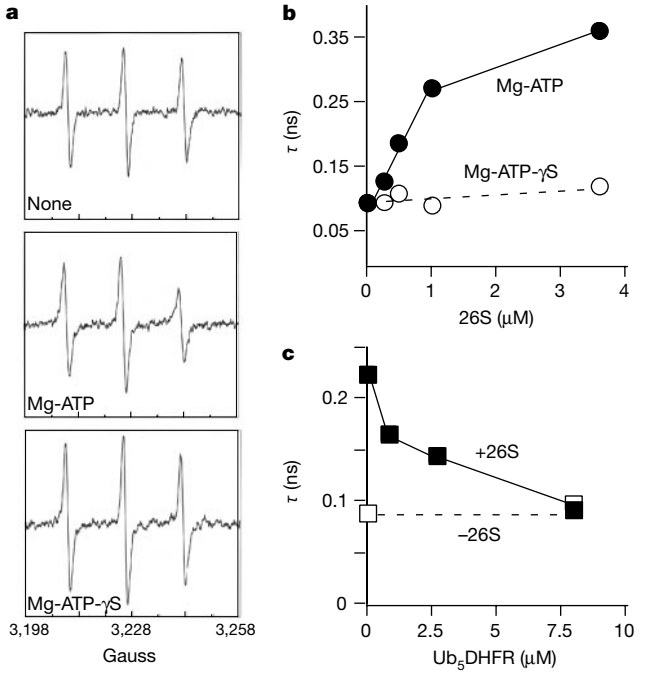

Figure 4 ATP hydrolysis modulates the polyubiquitin chain–proteasome interaction (EPR). **a**, Representative spectra. Incubations contained 2 μM Ub_4-proxyl; middle and lower panels also contained 3.6 μM 26S proteasomes with 1 mM Mg-ATP or ATP-γS (plus ATP regenerating system). **b**, Titration analysis. Incubations contained 2 μM Ub_4-proxyl, proteasomes and Mg-ATP or Mg-ATP-γS. **c**, Competition study. Incubations contained 1.7 μM Ub_5-proxyl, 2.7 μM proteasomes and Ub_5DHFR[6] as shown.

the bound polyubiquitin chain in a specific manner (Figs 2a, b and 3). However, Ub_4 did not bind detectably to recombinant glutathione *S*-transferase (GST)–Rpt5 in a pull-down assay (not shown), suggesting that the ability to form a functional chain-interaction site on S6′ is modulated by the presence of this subunit's neighbours within the 19S complex.

Consistent with identification of the S6′ ATPase as the subunit of the 19S complex that interacts with the polyubiquitin chain, efficient crosslinking to S6′ required ATP hydrolysis, as indicated by diminished crosslinking of the 50K protein in the presence of ADP or ATP-γS (Fig. 3d). A series of nucleoside 5'-triphosphates (NTPs) supported crosslinking in the order ATP ≈ CTP > GTP > UTP (Fig. 3d), similar to the NTPase specificity of the 19S complex[20]. ATP-γS is able to maintain the 19S–20S association (our own unpublished data and ref. 21); therefore, the diminished crosslinking signal seen in the presence of APT-γS (Fig. 3d) is not due to impaired proteasomal integrity. ATP hydrolysis may rather be necessary for efficient binding of the polyubiquitin signal to its cognate site. To address this possibility, we introduced a spin label (proxyl nitroxide coupled to maleimide) into Ub_4, and monitored its electron paramagnetic resonance (EPR) spectrum in the presence of proteasomes. In the absence of proteasomes, Ub_4-proxyl displayed a spectrum typical of a rapidly tumbling molecule (Fig. 4a, top panel). Upon addition of 26S proteasomes in the presence of Mg-ATP, the spectrum became more anisotropic, as demonstrated by the decreased ratio of the high field peak to the central peak, and the increased rotational correlation time (τ) (Fig. 4a, middle panel, and b). This effect was eliminated when ATP was replaced with ATP-γS (Fig. 4a, bottom panel, and b), providing direct physical evidence that the chain–proteasome interaction is modulated by ATP hydrolysis. To ensure that the chain binding site monitored in this experiment was functionally significant, we showed that the Mg-ATP-dependent increase in τ was competed efficiently by Ub_5DHFR (Fig. 4c), indicating that the chain-interaction site monitored by EPR is that which binds Ub_5DHFR with high affinity[6]. We note that even in the presence of proteasomes and Mg-ATP, the EPR signal of the spin-labelled chain is not characteristic of a highly immobilized molecule[22], suggesting that free and proteasome-bound chains are in rapid equilibrium. Consistent with this model, Ub_4 did not cosediment with 26S proteasomes on a glycerol gradient (our own unpublished data).

We have shown that a polyubiquitin chain interacts with the base of the 19S complex in a manner that places a critical region of the chain in close proximity to the S6′ ATPase (Figs 2 and 3). Moreover, ATP hydrolysis modulates the interaction between the chain and the proteasome (Figs 3d and 4). Competition by the 26S proteasome substrate Ub_5DHFR in crosslinking and EPR provides evidence that the site being monitored is that responsible for the recognition of polyubiquitinated substrates. These results implicate S6′ specifically, and the base of the 19S complex generally, in proteolytic signal recognition. S6′ is thus one of only a handful of 19S subunits with assigned functions. A specific role for this subunit in ATP-modulated polyubiquitin recognition is consistent with the ability of a non-proteasomal AAA ATPase to bind polyubiquitin chains[23], and may also help to explain the severe inhibition of model substrate degradation caused by a non-conservative mutation in the ATP-binding site of yeast Rpt5 (ref. 24). (However, because the ATPases probably form a ring, the effect of ATP on chain interaction could originate in the ATP site of a different ATPase.) Binding of the polyubiquitin signal to the base of the 19S complex should efficiently position the substrate for downstream events in proteolysis, as this subdomain also mediates substrate unfolding[7,9] and gating of the axial pore of the 20S complex[25]. A requirement for the lid of the 19S complex in the degradation of polyubiquitin-tagged substrates[8] may reflect as yet undiscovered interactions between a lid subunit(s) and the chain or substrate. Interestingly, the homogeneous ATPase subunits of the simpler archaebacterial and eubacterial proteasomes also mediate substrate recognition, usually by binding to a short motif within the substrate polypeptide chain[2]. Our results not only document a new role for ATP in polyubiquitin-dependent proteolysis, but also suggest that delegation of a signal-recognition function to a specific ATPase accompanied the functional diversification of these subunits in eukaryotes[24,25]. □

Methods

Antibodies and proteins

We purified 26S proteasomes from bovine erythrocytes[26]. Antibodies against S6 and S6′ were from Affiniti. We produced the antibodies against ubiquitin. Antibodies against Rpn10/S5a were a gift of R. Vierstra.

Reactive chains

Polyubiquitin chains were synthesized enzymatically[6,27]. APDP (*N*-[4-(*p*-azidosalicylamido)butyl]-3′-(2′-pyridyldithio)propionamide, 20 mM in DMSO; Pierce) was diluted to 3.4 mM in 35 μl of 0.15 M phosphate (pH 7.4) and radio-iodinated using chloramine-T (0.3 mCi of $Na^{125}I$ for 5 min, followed by 5 mM unlabelled KI). Ub_4 (proximal ubiquitin P37C, 4 mg ml^{-1}) was reduced with 0.5 mM dithiothreitol (30 min, 37 °C), diluted to 50 μM, incubated with ^{125}I-labelled APDP (2 mM, 1 h, 37 °C), and separated from unincorporated APDP on a spin column to yield APDP-Ub_4 at approximately 10^6 c.p.m. μg^{-1}. We used similar procedures to make reactive Ub_1. Reactive molecules were stored in the dark at 5 °C and used within 1 month.

Crosslinking

26S proteasomes (0.5 μM) were pre-incubated in the dark with reactive Ub_1 or Ub_4 (1 μM) for 10 min (10 μl, pH 7.6, 37 °C) in the presence of 0.5–2 mM Mg-ATP plus 1 μM ubiquitin aldehyde. To induce crosslinking, tubes were placed on an ultraviolet transilluminator for 2.5 min. Reactions were immediately quenched with SDS sample buffer (with or without mercaptoethanol as indicated) before resolution by SDS–PAGE.

EPR measurements

Maleimido-proxyl nitroxide (Aldrich) was reacted with Cys 37 (proximal) in Ub_4, and unincorporated spin label was removed by dialysis. EPR samples (5 μl) were loaded into capillary tubes with an internal diameter of 0.4 mm, and measurements were performed on a Bruker 300E spectrometer with loop-gap resonator at X-band using 1 mW microwave power[28]. In Fig. 4 spectra consisted of 25 or 50 summed 30-s scans. Each point in Fig. 4b was obtained by averaging 75 scans (from two experiments). In Fig. 4c, spectra consisted of ten scans (to prevent substantial degradation of Ub_5DHFR). We calculated rotational correlation times, τ, as described[22].

Received 17 December 2001; accepted 13 February 2002.

1. Hershko, A. & Ciechanover, A. The ubiquitin system. *Annu. Rev. Biochem.* **67,** 425–479 (1998).
2. Voges, D., Zwickl, P. & Baumeister, W. The 26S proteasome: a molecular machine designed for controlled proteolysis. *Annu. Rev. Biochem.* **68,** 1015–1068 (1999).
3. Chau, V. *et al.* A multiubiquitin chain is confined to specific lysine in a targeted short-lived protein. *Science* **243,** 1576–1583 (1989).
4. Finley, D. *et al.* Inhibition of proteolysis and cell cycle progression in a multiubiquitination-deficient yeast mutant. *Mol. Cell. Biol.* **14,** 5501–5509 (1994).
5. Pickart, C .M. Ubiquitin in chains. *Trends Biochem. Sci.* **25,** 544–548 (2000).
6. Thrower, J. S., Hoffman, L., Rechsteiner, M. & Pickart, C. M. Recognition of the polyubiquitin proteolytic signal. *EMBO J.* **19,** 94–102 (2000).
7. Braun, B. C. *et al.* The base of the proteasome regulatory particle exhibits chaperone-like activity. *Nature Cell Biol.* **1,** 221–226 (1999).
8. Glickman, M. H. *et al.* A subcomplex of the proteasome regulatory particle required for ubiquitin-conjugate degradation and related to the COP9-signalosome and eIF3. *Cell* **94,** 615–623 (1998).
9. Strickland, E., Hakala, K., Thomas, P. J. & DeMartino, G. N. Recognition of misfolded proteins by PA700, the regulatory subcomplex of the 26 S proteasome. *J. Biol. Chem.* **275,** 5565–5572 (2000).
10. Beal, R., Deveraux, Q., Xia, G., Rechsteiner, M. & Pickart, C. Surface hydrophobic residues of multiubiquitin chains essential for proteolytic targeting. *Proc. Natl Acad. Sci. USA* **93,** 861–866 (1996).
11. Vijay-Kumar, S., Bugg, C. E. & Cook, W. J. Structure of ubiquitin refined at 1.8 Å resolution. *J. Mol. Biol.* **194,** 531–544 (1987).
12. Cook, W. J., Jeffrey, L. C., Kasperek, E. & Pickart, C. M. Structure of tetraubiquitin shows how multiubiquitin chains can be formed. *J. Mol. Biol.* **236,** 601–609 (1994).
13. Beal, R. E., Toscano-Cantaffa, D., Young, P., Rechsteiner, M. & Pickart, C. M. The hydrophobic effect contributes to polyubiquitin chain recognition. *Biochemistry* **37,** 2925–2934 (1998).
14. Deveraux, Q., Ustrell, V., Pickart, C. & Rechsteiner, M. A 26 S protease subunit that binds ubiquitin conjugates. *J. Biol. Chem.* **269,** 7059–7061 (1994).
15. Fu, H. *et al.* Multiubiquitin chain binding and protein degradation are mediated by distinct domains within the 26 S proteasome subunit Mcb1. *J. Biol. Chem.* **273,** 1970–1981 (1998).
16. van Nocker, S. *et al.* The multiubiquitin-chain-binding protein Mcb1 is a component of the 26S proteasome in *Saccharomyces cerevisiae* and plays a nonessential, substrate-specific role in protein turnover. *Mol. Cell. Biol.* **16,** 6020–6028 (1996).
17. Hartmann-Petersen, R., Tanaka, K. & Hendil, K. B. Quarternary structure of the ATPase complex of human 26S proteasomes determined by chemical cross-linking. *Arch. Biochem. Biophys.* **386,** 89–94 (2001).
18. Davy, A. *et al.* A protein–protein interaction map of the *Caenorhabditis elegans* 26S proteasome. *EMBO Rep.* **2,** 821–828 (2001).

19. DeMartino, G. N. *et al.* Identification, purification, and characterization of a PA700-dependent activator of the proteasome. *J. Biol. Chem.* **271,** 3112–3118 (1996).
20. Hoffman, L. & Rechsteiner, M. Nucleotidase activities of the 26S proteasome and its regulatory complex. *J. Biol. Chem.* **271,** 32538–32545 (1997).
21. Verma, R. *et al.* Proteasomal proteomics: identification of nucleotide-sensitive proteasome-interacting proteins by mass spectrometric analysis of affinity-purified proteasomes. *Mol. Biol. Cell* **11,** 3425–3429 (2000).
22. Qin, P. Z., Butcher, S. E., Feigon, J. & Hubbell, W. L. Quantitative analysis of the isolated GAAA tetraloop/receptor interaction in solution: a site-directed spin labeling study. *Biochemistry* **40,** 6929–6936 (2001).
23. Dai, R. M. & Li, C.-C. H. Valosin-containing protein is a multi-ubiquitin chain-targeting factor required in ubiquitin-proteasome degradation. *Nature Cell Biol.* **3,** 740–744 (2001).
24. Rubin, C. M., Glickman, M. H., Larsen, C. N., Dhruvakumar, S. & Finley, D. Active site mutants in the six regulatory particle ATPases reveal multiple roles for ATP in the proteasome. *EMBO J.* **17,** 4909–4919 (1998).
25. Kohler, A. *et al.* The axial channel of the proteasome core particle is gated by the Rpt2 ATPase and controls both substrate entry and product release. *Mol. Cell* **7,** 1143–1152 (2001).
26. Hoffman, L., Pratt, G. & Rechsteiner, M. Multiple forms of the 20S multicatalytic and the 26S ubiquitin/ATP-dependent proteases from rabbit reticulocyte lysate. *J. Biol. Chem.* **267,** 22362–22368 (1992).
27. Piotrowski, J. *et al.* Inhibition of the 26 S proteasome by polyubiquitin chains synthesized to have defined lengths. *J. Biol. Chem.* **272,** 23712–23721 (1997).
28. Sankarapandi, S. & Zweier, J. L. Bicarbonate is required for the peroxidase function of Cu,Zn-superoxide dismutase at physiological pH. *J. Biol. Chem.* **274,** 1226–1232 (1999).

Acknowledgements

We thank G. DeMartino for a gift of modulator complex; A. Varshavksy for the GST–Rpt5 construct; A. Mildvan for discussions; and M. Hochstrasser and B. Cohen for comments on the manuscript. This work was supported by a grant from the National Institutes of Health. Y.A.L. is a senior fellow of the Leukemia and Lymphoma Society.

Competing interests statement

The authors declare that they have no competing financial interests.

Correspondence and requests for materials should be addressed to C.P. (e-mail: cpickart@jhmi.edu).

Geobacter metallireducens accesses insoluble Fe(III) oxide by chemotaxis

Susan E. Childers, Stacy Ciufo & Derek R. Lovley

Department of Microbiology, University of Massachusetts, Amherst, Massachusetts 01003, USA

Microorganisms that use insoluble Fe(III) oxide as an electron acceptor can have an important function in the carbon and nutrient cycles of aquatic sediments and in the bioremediation of organic and metal contaminants in groundwater[1,2]. Although Fe(III) oxides are often abundant, Fe(III)-reducing microbes are faced with the problem of how to access effectively an electron acceptor that can not diffuse to the cell. Fe(III)-reducing microorganisms in the genus *Shewanella* have resolved this problem by releasing soluble quinones that can carry electrons from the cell surface to Fe(III) oxide that is at a distance from the cell[3,4]. Here we report that another Fe(III)-reducer, *Geobacter metallireducens*, has an alternative strategy for accessing Fe(III) oxides. *Geobacter metallireducens* specifically expresses flagella and pili only when grown on insoluble Fe(III) or Mn(IV) oxide, and is chemotactic towards Fe(II) and Mn(II) under these conditions. These results suggest that *G. metallireducens* senses when soluble electron acceptors are depleted and then synthesizes the appropriate appendages to permit it to search for, and establish contact with, insoluble Fe(III) or Mn(IV) oxide. This approach to the use of an insoluble electron acceptor may explain why *Geobacter* species predominate over other Fe(III) oxide-reducing microorganisms in a wide variety of sedimentary environments[5–8].

Geobacter metallireducens, the first organism found to completely oxidize organic compounds to carbon dioxide with Fe(III) oxide serving as the electron acceptor[9–11], was previously reported to be non-motile[12]. However, in those previous studies, motility was evaluated in cultures grown on soluble electron acceptors such as nitrate or Fe(III)-citrate. We observed with phase-contrast microscopy that cells of *G. metallireducens* that had been grown on insoluble Fe(III) were motile. Furthermore, when we placed cells that had been grown on Fe(III) or Mn(IV) oxide onto soft agar plates they swam out from the line on which they were placed, whereas cells that had been grown on soluble Fe(III) did not (Fig. 1a).

Cells grown with insoluble Fe(III) or Mn(IV) oxides as the electron acceptor had lateral flagella that were apparent with transmission electron microscopy, whereas cells grown with soluble Fe(III) lacked flagella (Fig. 1b). Examination of 100 cells from each type of culture revealed that 77% and 68% of cells grown with

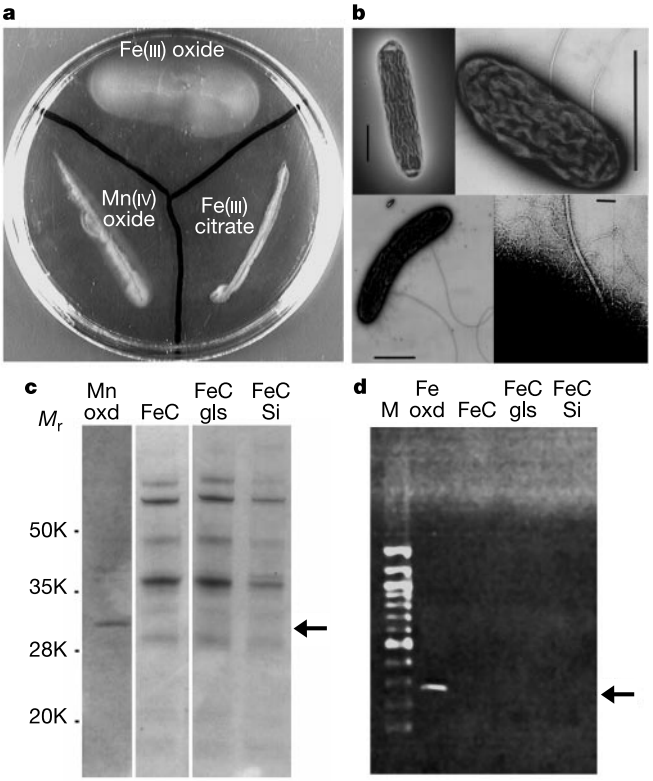

Figure 1 Expression of flagella and pili by *G. metallireducens*. **a**, Motility agar plate of swimming motility in response to growth with the electron acceptor indicated. A heavy suspension of cells was placed onto the plate and, after several days, the appearance of a light-grey haze extending outward from the initial streak indicated swimming. **b**, Electron micrographs showing the absence of flagella on cells grown with Fe(III)-citrate (top left), in contrast to cells grown with Fe(III) (top right) or Mn(IV) (bottom left) oxides as the terminal electron acceptor. Scale bars, 1 μm. The bottom right panel is a higher resolution electron micrograph of pili on cells. Scale bar, 0.1 μm. The contrast of the image was increased to enhance the visibility of pili. Cells were stained with 4% uranyl acetate and viewed with a JEOL 100S microscope. **c**, SDS–polyacrylamide gel electrophoresis of surface proteins obtained from *G. metallireducens* cells grown on Mn(IV) oxide (Mn oxd), Fe(III)-citrate (FeC), and Fe(III) citrate containing glass beads (FeC gls) or silica (FeC Si). The arrow points to the band consisting of flagellin protein. The molecular size standards are indicated on the left. **d**, PCR amplification of *pilA* from cDNA generated from mRNA. Cells were grown with the electron acceptor indicated (labelling as in **c**). Controls in which RNase was added to the reactions before reverse transcription was carried out showed no bands, indicating that the RNA preparation was not contaminated with DNA (not shown). The arrow points to te *pilA* PCR product. The marker (M) is a 1-kb DNA ladder (New England Biolabs).